International Journal of Civil Engineering and Technology (IJCIET)
Volume 10, Issue 01, January 2019, pp. 10-21, Article ID: IJCIET_10_01_002
Available online at http://www.iaeme.com/ijciet/issues.asp?JType=IJCIET&VType=10&IType=01
ISSN Print: 0976-6308 and ISSN Online: 0976-6316

STRENGTH AND STIFFNESS CHARACTERISTICS OF AXIALLY LOADED REINFORCED CONCRETE COLUMNS WITH DIFFERENT TYPES OF CONCRETE

Saad Khalaf Mohaisen*
Assistant Professor, Department of Civil Engineering, Al-Mustansiryah University, Baghdad, Iraq

Aamer Najim Abbas
Assistant Professor, Department of Civil Engineering, Al-Mustansiryah University, Baghdad, Iraq

Ali Sabah Ahmed
Associate Professor, Department of Civil Engineering, Al-Mustansiryah University, Baghdad, Iraq

ABSTRACT

The current paper is a report on the preparation and testing of 10 reinforced concrete column specimens of (120x120) mm^2 cross section and 1000 mm height, for the experimental clarification of the behavior of columns under the influence of pure axial loads. The research addresses the influences of some parameters and conditions on the mentioned behavior, including concrete type (normal strength, high strength or modified reactive powder concrete), the amount of reinforcement and the percentage of steel fibers. The effects of the above variables on the ultimate capacity, failure mode, stiffness, ductility and axial load-lateral displacement behavior were studied. It has been found that increasing the compressive strength and steel reinforcement ratio lead to increasing the ultimate capacity and stiffness of the tested columns. The effectiveness of increasing the steel fibers ratio is manifest in increasing the ultimate strength, ductility, and decreasing the stiffness and the ductility of the tested columns.

Key words: Axial load, RC column, reactive powder, high strength concrete, steel fibers.

Cite this Article: Saad Khalaf Mohaisen, Aamer Najim Abbas and Ali Sabah Ahmed, Strength and Stiffness Characteristics of Axially Loaded Reinforced Concrete Columns with Different Types of Concrete., International Journal of Civil Engineering and Technology, 10(01), 2019, pp. 10–21

http://www.iaeme.com/IJCIET/issues.asp?JType=IJCIET&VType=10&IType=01

1. INTRODUCTION

Previous works showed that the compressive strength, steel reinforcement, and dimensions of cross-sections of columns can directly affect the capacity of the column. There are many research works on using high strength concrete to advance the capacity of reinforced concrete columns [5, 12, 13]. Other researchers deals with the influence of transverse reinforcement proportion on the reinforced behavior of concrete columns [9, 15]. Later, researchers started to develop the strength characteristics of reinforced concrete columns through employing a special types of concrete [7, 8, 10] or external bonding by carbon fiber or steel plate [1, 2, 6, 11, 14]. The use of reactive powder concrete with a certain percentage of steel fibers to strengthen the reinforced concrete columns has not been widely investigated in the literature. This study will focus on the impacts of using different concrete types such; namely, high strength concrete , normal strength concrete, high strength concrete with different ratios of steel fibers and modified reactive powder concrete on the axially loaded reinforced concrete columns behavior.

2. DESCRIPTION OF SPECIMENS

Four types of concrete were employed in this research; namely, normal concrete, high strength concrete, high strength concrete with steel fibers and modified reactive powder concrete. All columns were of 120×120 mm^2 cross-sections and 1000 mm heights. Two different longitudinal reinforcement ratios were tackled in the present study, one case involved 4 ϕ8 mm bars and the other involved 8 ϕ8 mm bars. The spacing between stirrups was kept constant (ϕ6@100mm), see Table 1 below.

Table 1 Details of Specimens

Specimen No.	Dimensions (H×W×L) (mm^3)	Type of Concrete	Compressive Strength (MPa)	Reinforcement
C-1	120×120×1000	Normal	29.2	4 ϕ8 mm
C-2	120×120×1000	Normal	30	8 ϕ8 mm
C-3	120×120×1000	High strength	61.4	4 ϕ8 mm
C-4	120×120×1000	High strength	59.6	8 ϕ8 mm
C-5	120×120×1000	High strength with 1% steel fibers	60.8	4 ϕ8 mm
C-6	120×120×1000	High strength with 2% steel fibers	63.2	4 ϕ8 mm
C-7	120×120×1000	High strength with 1% steel fibers	61.1	4 ϕ8 mm

C-8	120×120×1000	High strength with 2% steel fibers	63.7	8 ϕ8 mm
C-9	120×120×1000	Reactive powder concrete	92	8 ϕ8 mm
C-10	120×120×1000	Reactive powder concrete	94	8 ϕ8 mm

3. MATERIALS

Below are the specifications and properties of materials used in this study:

3.1. Cement

Relevant chemical and physical features of the cement employed in the current work are given in Tables 2 and 3. The tests were conducted according to ASTM C-150 [3].

Table 2 Chemical installation of Cement

Chemical installation	Percentage by weight
CaO	53.2
SiO_2	24.4
Al_2O_3	6.3
Fe_2O_3	3.19
MgO	3.08
SO_3	1.72
L.O.I	2.1
I.R	0.92
L.S.F	0.88
CaO	53.2

Table 3 Physical Features of Cement

Physical Feature	Result of test
Fineness (kg/m^2)	2930
Soundness	0.24%
Initial setting time (min.)	143
Final setting time (min.)	211
Compressive strength (3 days) (MPa)	11.3
Compressive strength (7 days) (MPa)	17.5
CaO	53.2

3.2. Fine Aggregate

In this research a fine aggregate maximum size was 5 mm. The fine aggregate properties are demonstrated in Tables 4 and 5.

Table 4 Fine Aggregate Grading

Sieve size (mm)	Present work of fine aggregate (% passing)	BS882:1992 Limit zone “M” (%passing)[4]
10	100	100
5	90.19	89-100
2.36	87.29	65-100
1.18	47.21	45-100
0.6	53.21	25-80
0.3	39.93	5-48
0.15	11.02	0-15

Table 5 Physical properties of fine aggregate

Sieve size (mm)	BS882:1992 Limit zone “M” (%passing)[4]
Water absorption	0.55%
Specific gravity	2.41%
Fineness modulus	2.73%
Moisture content	0.26%

3.3. Coarse Aggregate

A maximum size of 10 mm crushed coarse aggregate was used in the present experimental program. Table 6 shows the grading of coarse aggregate.

Table 6 Coarse Aggregate Grading

Sieve size (mm)	Present work of coarse aggregate (% passing)	BS882:1992 Limit (%passing)[4]
20	100	100
14	100	90-100
10	77.1	50-85
5	7.8	0-10
2.36	0	0

3.4. Steel Reinforcements

Tensile test of steel reinforcement was carried out on ϕ8 mm deformed mild steel bar put as a flexural reinforcement, and ϕ6 mm deformed mild steel bar was put as shear reinforcement. Table 7 shows the results of tensile test for those bars.

Table 7 Properties of steel bars

Nominal Diameter (mm)	Bar Type	f_y (MPa)	f_u (MPa)	E_s (GPa)	Elongation %
8	Deformed	397	538	200	10.3
6	Deformed	414	623	200	11.4

3.5. Silica Fume

Table (8) presents the specifications done by manufacturer of silica fume used in this study.

Table 5 Physical features of fine aggregate

Property	Result
State	Sub-micro Powder
Colour	Grey to Medium Grey
Specific Gravity	2.10 to 2.4
Bulk Density	500 to 700 kg/m3
Chemical Requirements: Silicon Dioxide (Sio2) Water Amount (H2O) Loss of Ignition (LOI)	 Minimum 85% Maximum 3% Maximum 6%
Physical Requirements: Specific Surface Area Pozzolanic Activity Index, 7-days Over Size Particles Retained on 45 Micro Sieve	 Minimum 15 m2/g Maximum 105% of Control Maximum 10%

3.6. Steel Fibers

Table 9 presents the specifications done by manufacturer of steel fibers used in the present work.

Table 9 Specifications of Steel Fibers

Specification	Result
Appearance	Bright Grey Metal Fibers
Color Essentially	Odorless
PH	N/A
Melting Point	2700 ^{O}F (1482^{O}C)
Solubility in Water	Insoluble
Specific Gravity	7-8 gram/cm^3
Vapor Density	N/A
Boiling Point	N/A
% Solid	100%
Flash Point	N/A
Auto Ignition Temp	N/A

3.7. Super-plasticizer

Table 10 presents the descriptions done by manufacturer of the Super-plasticizer used in this study.

Table 10 Descriptions of Super-plasticizer

Specification	Result
Form	Viscous Liquid
Colour	Light Brown
Relative Density	1.1@20^{O}C
PH	6.6
Viscosity	128+/-30 CPS@20^{O}C

4. CRACK PATTERNS AND FAILURE MODES

Figure 1 below shows the observed crack patterns and modes of failure for the four types of concrete experimented upon in the present work, and explains the differences in the more plausible failure processes affecting each one of them. After initiation of cracks at the core cover interface, the concrete cover spalled out at the ends of the specimen when the advanced stages of loading application were reached.

It is also observed that the cracks on the column surface in modified reactive powder concrete are mainly straight without significant secondary cracking.

By observing the ends of the columns after failure, it could be seen that the 90-degree hooks in the columns had a tendency to split up for all tested specimens. The deformation of those 90-degree hooks is thought to be the main factor initiating cover spalling.

Column C-1

Column C-2

Column C-3

Column C-4

Column C-5

Column C-6 **Column C-7** **Column C-8** **Column C-9** **Column C-10**

Figure 1 Failure Modes of Tested Columns

5. ULTIMATE FAILURE LOAD

The use of high strength concrete, such as high-performance concrete or reactive powder concrete achieve to a large extent in carrying capacity of specimens, and that is what reached in this study.

The ultimate capacity of tested the specimens was affected by increasing the compressive strength. Improvement of the ultimate capacity of specimens C-3 and C-4 were about 40.9% and 38.36% respectively in comparison with the corresponding normal strength concrete columns C-1 and C-2.

As is intuitively expected, increasing the steel fiber ratio had a positive effect on the ultimate capacity of the tested columns. This is plainly evident when recalling that the ultimate strength improved by about 22.5% and 11.8% of specimens C-5 and C-7 upon using 1% steel fibers in comparison with the reference specimens C-3 and C-4 respectively. The ultimate capacity of the specimens with 2% steel fibers improved to about 37% and 10% in comparison with high strength concrete specimens free of steel fibers.

This improvement is plausibly attributed to the bridging effect that results from the presence of the steel fibers, which connects both sides of a crack and decelerates the development of crack width [16].

The improvement of carrying capacity of modified reactive powder concrete columns among other types is due to the increasing depth of the neutral axis and increasing the static modulus of elasticity of modified reactive powder concrete specimens [15].

The efficacy of increasing the steel reinforcement ratio can be seen clearly in specimens C-2, C-4, C-7, C-8 and C-10 which the amount of improvement reached to 80.6%, 77.42%, 61.84%, 42.35% and 12.32% over reference specimens C-1, C-3, C-5, C-6 and C-9 respectively. The increase of the total capacity is thought to has been induced by the improvement of moment resisting resulting from the increase of steel reinforcement ratio, see Table 11.

Table 11 Ultimate and Cracking Loads

Sample No.	Load of Cracking (kN)	Load of Yielding (kN)	Load of Ultimate (kN)
C-1	120	180	220
C-2	300	350	397.5
C-3	240	260	310
C-4	430	500	550
C-5	290	350	380
C-6	350	560	425
C-7	490	410	615
C-8	510	570	605
C-9	420	500	527.5
C-10	540	520	592.5

6. THE BEHAVIOR OF AXIAL LAD-LATERAL DISPLACEMENT

By studying the behavior of the displacement of axial load-lateral curves of all tested columns in Figures (2) to (11), it turns out that there are three basic stages, each stage reflects the behavior of the loaded member under the influence of the applied loading. The first stage characterized by linear relationship between load and lateral displacement, starts at the beginning of load application until appearance of first crack. The specimen behaves elastically. In other word, the specimen back to original manner when releasing the load. Then the second stage starts and extends until the yielding of steel reinforcement bars. At the end of this stage, the specimen has lost most of its stiffness. The third non-linear stage begins after the yielding of steel bars commences and continues up to failure. At this stage, it has been observed that the rate at which the deformations of normal strength concrete specimens increases is slower than that of the high strength concrete specimens. The use of steel fibers achieved positive results in control on the deformations rating of high strength concrete.

Table 11 contains a comparison between the values of cracking loads and yielding loads of different specimens. It is clear that the increase of compressive strength results an increase in the value of cracking load up to about 91.6 and 266.6 % in columns C3 and C9, respectively, in comparison with reference specimen C1. Also, increasing compressive strength delays the yielding of steel bars up to about 44.5 and 177.7% in columns C3 and C9, respectively, in comparison with reference sample C1.

The steel fibers positively effect on the appearance of first crack. the value of improvement about 20.8% and 104.16% in specimens C5 and C7 respectively which have 1% steel fibers over reference specimen C3. Also, the amount of improvement about 45.83% and 112.5% in specimens C-6 and C-8 respectively which have the 2% steel fibers over reference specimen C-3.

The yielding load also affected by using steel fiber by about 34.6 and 57.7 % in columns C5 and C7 respectively and about 115.38% and 119.23% in columns C-6 and C-8 respectively in comparison with reference column C3.

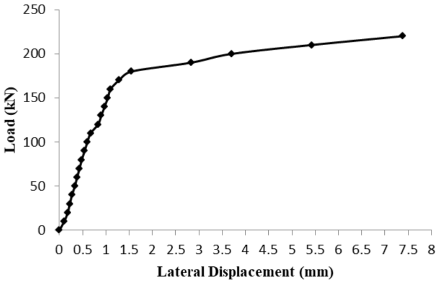

Figure 2 Load-lateral Displacement Curve for Sample C-1

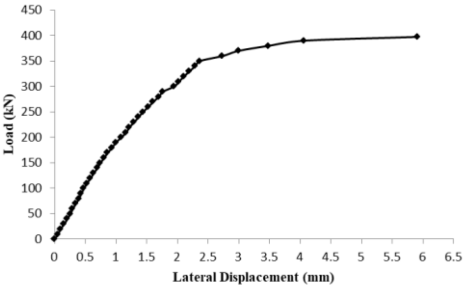

Figure Load-lateral Displacement Curve for Sample C-2

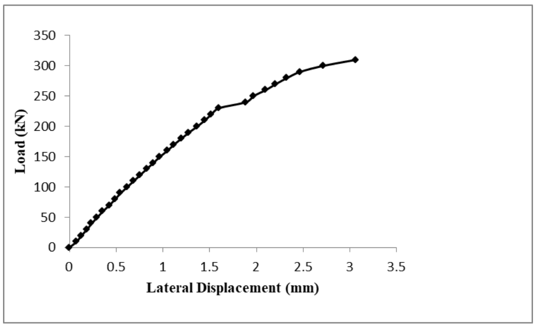

Figure 4 Load-lateral Displacement Curve for Sample C-3

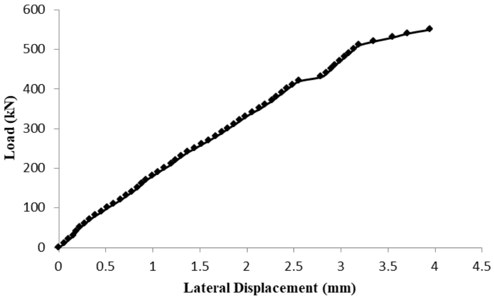

Figure 5 Load-lateral Displacement Curve for Sample C-4

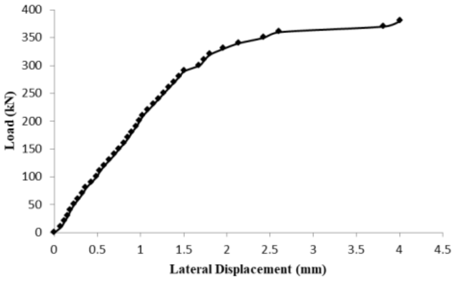

Figure 6 Load-lateral Displacement Curve for Sample C-5

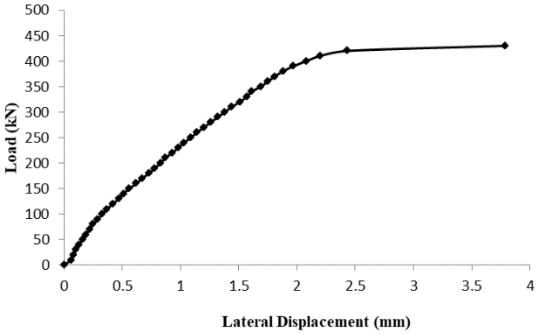

Figure 7 Load-lateral Displacement Curve for Sample C-6

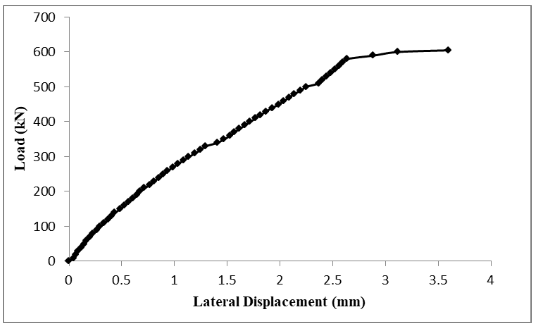

Figure 8 Load-lateral Displacement Curve for Sample C-7

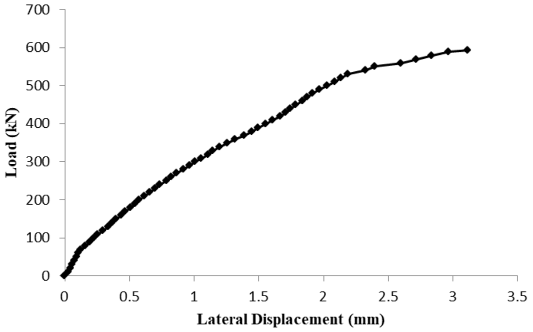

Figure 9 Load-lateral Displacement Curve for Sample C-8

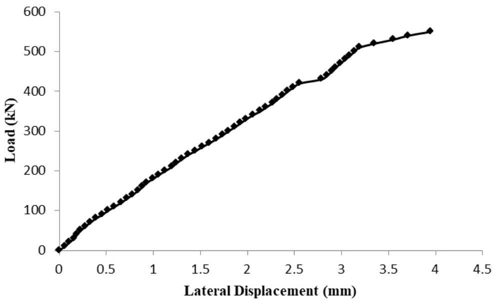

Figure 10 Load-lateral Displacement Curve for Sample C-9

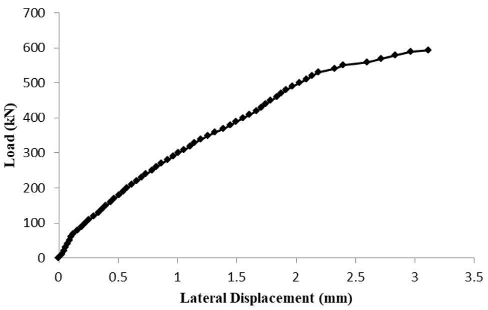

Figure 11 Load-lateral Displacement Curve for Sample C-10

7. STIFFNESS

Improvement in stiffness is shown in Table 12. The stiffness of column specimens increases as the compressive strength and longitudinal reinforcement ratio increase because the decreasing of carrying capacity was accompanied by a decrease of the amount of deflection. Unlike the steel fiber reinforced concrete columns, the stiffness decreases when using steel fibers as indicated by the increase in deflection at failure.

Through observation of the displacement of load-lateral curve, it can be seen that there was a decrease in stiffness with the gradual increase of the applied load, as shown in Table 12, where the stiffness of the tested specimens at load of first cracking is greater than the stiffness at load of yielding, and the latter is greater than the stiffness at failure.

Table 12 Stiffness of Tested Columns

Sample No.	Stiffness at Cracking Load (kN/m)	Stiffness at Yielding Load (kN/m)	Stiffness at Failure (kN/m)
C-1	144.57	116.12	29.81
C-2	153.84	147.67	67.14
C-3	143.75	123.8	100.97
C-4	154.12	149.23	139.24
C-5	192	144	94.76
C-6	176.53	174.45	113.13
C-7	207.1	186.36	161
C-8	215.18	209.23	168
C-9	209.52	196.1	157
C-10	251.46	243	189.9

8. SPECIMENS CURVATURE DUCTILITY

The deformability of structural members under earthquakes load depends mainly on its ductility (the ability of the member to deform inelastically without a significant loss of strength). The curvature ductility factor can be found using the relationship ($\mu\varphi u/\varphi y$) where (φu) and (φy) are the curvature angles at fracture and at steel yielding respectively.

By observing the Table 13, shows that the ductility decreased with increasing the longitudinal reinforcement ratio and compressive strength, so the failure is sudden in modified reactive powder concrete and high strength concrete. On the contrary, increasing the proportion of steel fibers results in increasing the ductility of tested specimens, because of the steel fibers overlap with concrete mortar effects on reducing the rate of deformation in the advanced stages of loading application.

Table 13 Curvature Ductility of Tested Columns

Sample No.	$\Phi u \times 10^{-3}$	$\varphi y \times 10^{-3}$	Curvature ductility (μ)
C-1	845	177	4.77
C-2	678	271	2.5
C-3	352	240	1.46
C-4	452	359	1.26
C-5	459	278	1.65
C-6	437	312	1.4
C-7	434	252	1.72
C-8	412	298	1.38
C-9	385	292	1.32
C-10	357	245	1.45

9. CONCLUSIONS

The results of tests indicated:

1. The failure of normal reinforced concrete columns is more controllable than the failure in high strength and modified reactive powder concrete columns.
2. The usage of modified reactive powder concrete and high strength concrete enhanced the ultimate capacity of the tested samples.
3. The use of steel fibers improved the ultimate strength.
4. The effectiveness of increasing the longitudinal steel reinforcement proportion is clear in increasing the capacity of ultimate reinforced concrete columns.
5. Increasing the compressive strength, longitudinal reinforcement the steel fibers proportion and percentage led to an increasing in the capacity of cracking of the tested columns.
6. Stiffness of the tested columns increase with the increasing of concrete compressive strength and longitudinal reinforcement ratio and decreased with the increase of steel fibers percentage.
7. The deformability of the tested columns under loading application decreased with increasing the longitudinal reinforcement ratio and compressive strength. Furthermore, increasing the percentage of steel fibers made the specimens failed in ductile mode.

REFERENCES

[1] Abdelrahman, K, and El-Hacha, R. Cost and ductility effectiveness of concrete columns strengthened with CFRP and SFRP sheets. Polymers, 6(5), 2014, pp. 1381.

[2] Al-Karaghool, H. O. Strength and ductility of axially loaded RC short columns confined with CFRP and GFRP wraps. Master's thesis, American University of Sharjah, 2013.

[3] Standard Specifications for Portland cement. ASTM C-150, ASTM International, 2015.

[4] Specifications for Aggregate from Natural Source for Concrete. BS 882-1992, British Standards Institution, 1992.

[5] Chikh, N., Gahmous, M. and Benzaid, R. Structural performance of high strength concrete columns confined with CFRP sheets. In Proceedings of the World Congress on Engineering, volume 3, 2012.

[6] Mote, A. P. and Jadhav, H. S. Experimental study of axially loaded RC short columns strengthened with basalt fiber reinforced polymer (BFRP) sheets. Int. Journal of Engineering Research and Applications, 2014, pp. 2248-9622.

[7] Nandhinisree, M. and Saravana Kumar, N. Structural behavior of self-compacting concrete confined with ferrocement under axial compression. SSRG International Journal of Civil Engineering, 1(1), 2014, pp. 24.

[8] Omar, M. M., Gomes, R. B., and Abreu Reis, A. P. Experimental analysis of reinforced concrete columns strengthened with self-compacting concrete. Revista IBRACON de Estruturas e Materiais, 3(3): 2010, pp. 271.

[9] Pallewatta, T. M., Irawan, P. and Maekawa, K. Effectiveness of laterally arranged reinforcement on the confinement of core concrete. Doboku Gakkai Ronbunshu, 1995(520), 1995, pp. 297.

[10] Paultre, P., Khayat, K. H, Cusson, D., and Tremblay, S. Structural performance of self-consolidating concrete used in confinement of concrete columns. ACI structural journal, 102(4): 2005, pp. 560.

[11] Rocca, S., Galati, N. and Nanni, A. Large-size reinforced concrete columns strengthened with carbon FRP: Experimental evaluation. In Proceedings of the Third International Conference on FRP Composites in Civil Engineering. Miami, USA, December, 2006, pp. 491-494.

[12] Sungjoong, K. Behavior of High Strength Concrete Columns. PhD thesis, North Carolina State University, 2007.

[13] Hassan and Kadhim Naief Kadhim (Development an Equation for Flow over Weirs Using MNLR and CFD Simulation Approaches). (IJCIET), Volume 9, Issue 3, (Feb 2018)

[14] Yang, K. and Ashour, A. F. Tests of reinforced concrete short columns laterally strengthened with wire rope units and steel elements, 2007.

[15] Ziehl, P. H. Cloyd, J. E. and Kreger, M. E. Evaluation of minimum longitudinal reinforcement requirements for reinforced concrete columns. Center for Transportation Research, Bureau of Engineering Research, University of Texas at Austin, 1998.

[16] Waryosh, W. A., Mohaisen, S. K. and Dkhel, R. H. Deformation responses of reinforced concrete beams under pure torsion. IOP Conf. Series: Materials Science and Engineering, 433: 2018.